Truncated Battery Power Following Strategy for Energy Management Control of Series Hybrid Electric Vehicles

Boli Chen and Simos A. Evangelou

***Abstract*— This paper deals with the optimal energy management control of series hybrid electric vehicles (HEVs) by which their fuel consumption is minimized. Based on the modeling of the essential dynamics of a series HEV and its powertrain, closed-form solutions of the optimal energy source power split are formulated. These solutions yield a set of simple heuristic control rules, by which a novel rule-based control strategy, the truncated battery power following strategy (TBFS), is developed for optimally allocating the hybrid energy sources to satisfy the demanded propulsion power. Numerical examples show that the TBFS is able to reproduce the globally optimal solutions found by dynamic programming (DP), but with significantly reduced computation effort, as the TBFS only requires one-dimensional parameter tuning, rather than solving an optimization problem. The results also indicate its benchmark potential for high-fidelity HEV models, where DP is no longer applicable.**

I. Introduction

Commonly, the hybrid electric vehicle (HEV) is a combination of an internal combustion engine (ICE) and a battery-driven electric motor. As such, HEVs can profit from a freely optimized power split between the two energy sources for improving fuel economy as compared to conventional vehicles. The problem of finding a fuel-efficient power split for HEVs has received substantial research efforts in the past [1], [2]. Numerous energy management (EM) control strategies, from rule-based to optimization-based strategies, have been proposed in the literature.

Optimization-based EM strategies represent the most commonly used benchmark methods as optimal or sub-optimal solutions are guaranteed in most cases. The EM problem in this category is usually formulated as an optimal control problem (OCP), which is then solved by standard optimization techniques. Dynamic programming (DP) represents the most commonly used solution method, which usually ensures global optimality [3]–[5]. However, it is limited to highly simplified models as the computation burden increases exponentially with the number of system states [6]. Many alternative algorithms are developed by suitable approximations of the global optimization problem, such as the Pontryagin Minimum Principle (PMP) based approaches and the equivalent consumption minimization strategy (ECMS) [7]–[10]. These approaches substantially reduce the computational burden at the price of yielding suboptimal solutions. In contrast with DP, both PMP and ECMS can be potentially implemented in real-time [11]–[13].

Heuristic control techniques are usually characterized by Boolean or fuzzy rules, which mostly depend on the HEV powertrain architecture. In terms of the series HEV that is the focus of the present work, thermostat control strategy (TCS) and power follower control strategy (PFCS) represent the two most conventional rule-based controllers designed for series HEVs, yet their fuel economies are not optimized. By considering the most effective design principles of TCS, PFCS and the optimization-based ECMS, the heuristic method exclusive operation strategy (XOS) is recently proposed to reduce the performance gap with optimization-based solutions [14]. Even though it outperforms existing heuristic strategies, the XOS is still falling behind optimization-based benchmarks by some margin.

The present work proposes a novel heuristic EM strategy, the truncated battery power following strategy (TBFS), which is constructed by simple and effective rules. The rules are extracted from the optimal energy management control problem analytic solution, which is derived in this work for an elementary but widely used and applicable series HEV model [11], [15], [16]. The devised heuristic strategy thus allows the optimal EM solution to be reached without solving any optimization problem, but merely by a single tunable parameter, which demands very slight tuning effort. The performance of the proposed EM strategy is evaluated and compared with DP in numerical examples.

The remainder of the paper is structured as follows. Section II introduces the vehicle model and formulation of the EM problem. A theoretical study of the optimal EM solutions is presented in Section III, and from the analysis and derived solutions, a novel heuristic EM control strategy is proposed. Simulation results, involving a comparison with DP solutions, and discussion are presented in Section IV. Finally, concluding remarks are given in Section V.

II. Problem Description

A. Vehicle Model

The vehicle studied in this work is a mid-size car with a series HEV powertrain that is sketched in Fig. 1. As it

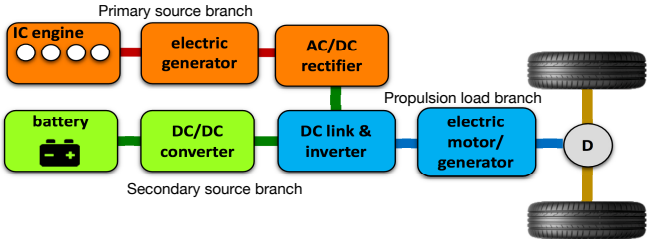

Fig. 1. Block diagram of the series HEV powertrain.

can be seen, the three powertrain branches: primary source branch (PS), secondary source branch (SS) and propulsion load branch (PL) are coupled electrically at the DC-link, such that the demanded PL branch power P_{PL} is met by the combination of the PS output power P_{PS} and the SS output power P_{SS}:

$$P_{PL} = P_{PS} + P_{SS}. \tag{1}$$

B. Chen and S. A. Evangelou are with the Dept. of Electrical and Electronic Engineering at Imperial College London, UK (boli.chen10@imperial.ac.uk, s.evangelou@imperial.ac.uk).

This research was supported by the EPSRC Grant EP/N022262/1.

1) Propulsion Load Branch: For a given speed profile specified in terms of speed v and acceleration a, the driving force acting on the wheels is available, obtained as follows:

$$F_{drive} = m\,a + F_T + F_D + mg\sin\theta, \tag{2}$$

in which m is the vehicle mass, $F_T = f_T\,m\,g$ and $F_D = f_D v^2$ are the resistance forces respectively due to tires and the aerodynamics drag, and θ is the road slope associated with the speed profile. f_T and f_D are the coefficients of tire rolling and aerodynamics drag resistances, which are specified in Table I.

In this work, the electric motor efficiency is described by a static efficiency map, as shown in Fig. 2. The motor speed

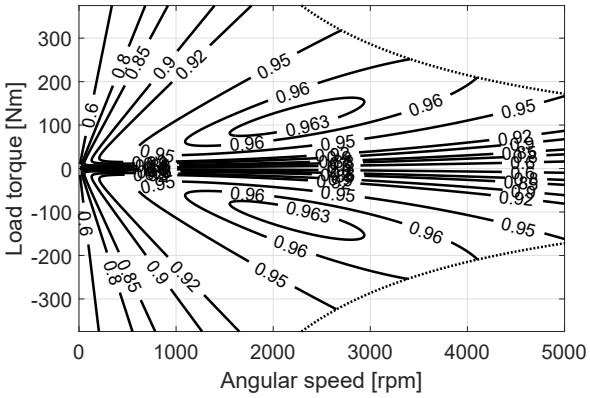

Fig. 2. Efficiency of the reversible PMS machine (generator = positive torque, motor = negative torque). The torque bounds (due to power limitation) are shown by dotted lines.

ω_m is coupled with the speed of the wheels (i.e., vehicle speed v) by a transmission system with single fixed gear ratio g_t, such that $\omega_m = \mathrm{g}_t v$.

It is clear that the operation of the PL branch is allowed to be isolated from the EM strategy. As such, the load power demand P_{PL} at the DC-link can be calculated directly from the power at the wheels, P_{drive}, as follows:

$$\begin{cases} P_{PL} = \dfrac{P_{drive}}{\eta_i\eta_m\eta_t}\,, \forall\, P_{drive} \geq 0\,, \\ P_{PL} = \max\left(P_{drive}\eta_i\eta_m\eta_t,\, P_{SS_{\min}}\right)\,, \forall\, P_{drive} < 0\,. \end{cases} \tag{3}$$

where $P_{drive} = F_{drive}\,v$ is determined by the driving cycle and longitudinal car dynamics, $P_{SS_{\min}}$ represents the SS maximum charging power, and η_i, η_m, η_t are the efficiency of the inverter, motor and the transmission, respectively. It should be noted that the second equation in (3) relies on the assumption that all the braking energy is recoverable (not restricted by the braking distribution between front and rear axles) and it is only restricted by $P_{SS_{\min}}$. In this context, the mechanical braking power is as follows: $P_h = \min\left(0, P_{drive} - P_{SS_{\min}}/(\eta_i\eta_m\eta_t)\right)$, which is naturally minimized as P_h is dissipated as heat.

To sum up, for a given driving cycle, P_{PL} can be considered as the reference to be followed instead of the driving cycle. As such, optimal energy management fulfills minimization of fuel consumption by means of an appropriate power split between PS and SS to satisfy P_{PL}.

2) Primary Source Branch: The primary source branch from the ICE to the AC-DC rectifier is modeled as a steady state efficiency map, which is simply obtained as the product of individual component efficiencies, where the same electric machine as that in Fig. 2 is used for the generator. The fact that there is no mechanical connection between the engine and the vehicle wheels allows the crankshaft speed to be freely assigned independently of the vehicle speed. By operating the engine branch along the locus of most efficient power-speed operating points, the engine fuel mass rate is usually approximated as a linear function of P_{PS}, as follows:

$$\frac{d}{dt}m_f = q_{f0} + \alpha_f P_{PS} \tag{4}$$

where q_{f0} acts as the idling fuel mass rate, and α_f is the coefficient of power transformation. These two positive parameters are directly obtained by linear regression of the steady state engine data when the most efficient torque-speed operating point is followed at each power value. An example is illustrated in Fig. 3, where the engine map utilized is for the Audi 5-Cylinder Turbo Diesel Engine taken from the Advanced Vehicle Simulator (ADVISOR) [17]. As it can be noticed, the nonlinear relationship between $\dot{m}_f$ and P_{PS} is accurately fitted by a linear fuel consumption model (FCM).

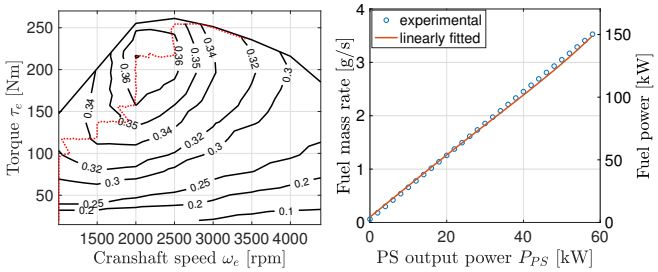

Fig. 3. Left: map of overall efficiency of the engine branch. The torque-speed operating points for maximum engine branch efficiency at different output power values are shown by a dashed curve. Right: fuel mass rate with PS power, when the most efficient torque-speed operating point is followed at each power value.

3) Secondary Source Branch: The battery is modeled as a series connection of an ideal voltage source and an ohmic resistance [11]. Therefore, the battery output power P_b is calculated as follows:

$$P_b = (V_{oc} - i_b R_b) i_b, \tag{5}$$

in which V_{oc} is the battery open-circuit voltage, i_b denotes the battery current, and R_b is the internal resistance. The battery state-of-charge (SOC) represents the only state variable, governed by:

$$\frac{d}{dt}\mathrm{SOC} = -\frac{i_b}{Q_{\max}}\,, \tag{6}$$

where $Q_{\max}$ is the battery capacity and i_b is assumed positive during the discharge phase. By using (5), the battery current can be solved as follows:

$$i_b = \frac{V_{oc} - \sqrt{V_{oc}^2 - 4P_b R_b}}{2R_b}\,. \tag{7}$$

Instead of using a nonlinear mapping between SOC and the open circuit voltage (as it is known in the literature), V_{oc} is reasonably approximated by a constant voltage, which is compatible with the usual aim of a charge sustained battery management, by which the SOC is narrowly constrained. Furthermore, by combining the battery with the bidirectional DC/DC converter, the SS output power is obtained by:

$$P_{SS} = \eta_{dc}^{\mathrm{sign}(P_{SS})} P_b, \tag{8}$$

where η_{dc} is the efficiency of the DC/DC converter. Substituting the algebraic solution of i_b (obtained by applying (8) in (7)), the dynamic behavior of the SS can be described by the differential equation of SOC with respect to P_{SS} only:

$$\frac{d}{dt}\mathrm{SOC} = \frac{-V_{oc} + \sqrt{V_{oc}^2 - 4P_{SS}\, R_b/\eta_{dc}^{\mathrm{sign}(P_{SS})}}}{2R_b\, Q_{\max}}\,. \quad (9)$$

B. Problem Formulation

According to the power balance at DC-link (1), the input power signal P_{PS} of the FCM (4) can be replaced by P_{SS}. Thus, the overall vehicle system is constructed with only a single input, as follows:

$$\frac{d}{dt}\mathbf{x} = \mathbf{f}(\mathbf{x},\mathbf{u}) = \begin{pmatrix} q_{f0} + \alpha_f(P_{PL} - P_{SS}) \\ \dfrac{-V_{oc} + \sqrt{V_{oc}^2 - 4P_{SS}\, R_b/\eta_{dc}^{\mathrm{sign}(P_{SS})}}}{2R_b\, Q_{\max}} \end{pmatrix}. \quad (10)$$

where $\mathbf{x} \triangleq [m_f, \mathrm{SOC}]^\top$ and $\mathbf{u} \triangleq P_{SS}$ represent the state variables and the control input, respectively.

Consider T the total time duration of the driving mission. The EM control of an HEV aims to minimize the overall fuel consumption $m_f(T)$ by properly selecting P_{SS}, subject to the SOC operational limits:

$$\mathrm{SOC}_{\min} \le \mathrm{SOC} \le \mathrm{SOC}_{\max}\,, \quad (11)$$

and the energy source power limits:

$$P_{SS_{\min}} \le P_{SS} \le P_{SS_{\max}} \quad (12)$$

$$0 \le P_{PS} \le P_{PS_{\max}} \quad (13)$$

where $P_{PS_{\max}}$ and $P_{SS_{\max}}$ are the maximum propulsive power PS and SS can deliver. Resorting to (1) the power limits (12) and (13) can be combined and implemented as a constraint only on the SS power output P_{SS}, as follows:

$$\max(P_{PL} - P_{PS_{\max}},\, P_{SS_{\min}}) \le P_{SS} \le \min(P_{SS_{\max}}, P_{PL})\,. \quad (14)$$

In addition to (11), the EM also targets charge sustaining operation:

$$\Delta\mathrm{SOC} \triangleq \mathrm{SOC}(0) - \mathrm{SOC}(T) = 0. \quad (15)$$

It is worth noting that the described EM control problem can be naturally formulated as an optimization problem with only one dynamic state, the SOC, since the linear dependence of the fuel consumption rate on the PS power enables an alternative objective $\min \int_0^T (P_{PL} - P_{SS})dt$ to be used instead of $\min m_f(T)$. As such, the fuel usage is allowed to be evaluated a posteriori based on the optimal solution. Such single state optimization problem makes DP a very effective tool for obtaining its globally optimal solution.

The main characteristic parameters of the vehicle model are summarized in Table I. Note that the battery and engine power limits are chosen to emulate the energy sources for a non-plug-in HEV.

TABLE I
MAIN VEHICLE MODEL PARAMETERS

symbol	value	description
m	1500 kg	vehicle mass
f_T	0.01	rolling resistance coefficient
f_D	0.47	aerodynamics drag coefficient
η_t	0.96	efficiency of the transmission
g_t	10	transmission ratio
q_{f0}	0.12g/s	idling fuel mass rate
α_f	0.059g/kW/s	power transformation factor
$Q_{\max}$	5 Ah	battery capacity
R_b	0.2056 Ω	battery internal resistance
V_{oc}	300 V	battery open circuit voltage
η_r, η_i	0.96	efficiency of inverters
η_{dc}	0.96	efficiency of converter
$P_{SS_{\min/\max}}$	−15/30kW	SS power limit
$\mathrm{SOC}_{\min/\max}$	0.5/0.8	battery SOC limits
$P_{PS_{\max}}$	70kW	PS power limit

III. Energy management strategies based on the fundamental analysis of fuel efficiency optimization

This section provides a fundamental analysis to show the nature of optimal energy management solutions for the presented series HEV model (10). The analysis provides an explicit condition for optimality, which yields the fundamental rules of the proposed TBFS. To proceed with the analysis, let us first introduce some useful notations and definitions for the upcoming analysis. Consider two sets of time intervals $\Phi \triangleq \{t|P_{PL}(t) \ge 0\}$ and $\Psi \triangleq \{t|P_{PL}(t) < 0\}$, such that $\Phi \cup \Psi$ is the full time horizon $\{t|0 \le t \le T\}$. Moreover, it is immediate to obtain the power-sharing pattern for $t \in \Psi$:

$$P_{PS} = 0, \quad P_{SS} = P_{PL}. \quad (16)$$

Analogously, Φ can be divided into two subsets as $\Phi = \Phi_d \cup \Phi_c$, where $\Phi_d \triangleq \{t|P_{PL}(t) \ge 0, i_b(t) \ge 0\}$ and $\Phi_c \triangleq \{t|P_{PL}(t) \ge 0, i_b(t) < 0\}$. These subsets respectively collect the battery discharging and the charging intervals for all $t \in \Phi$. Moreover, define the battery internal power: $P_{oc} \triangleq V_{oc}\, i_b$. Then the battery efficiency is expressed as:

$$\eta_b(t) = \begin{cases} \dfrac{P_b(t)}{P_{oc}(t)} = 1 - \dfrac{R_b}{V_{oc}^2} P_{oc}(t), & \text{if } t \in \Phi_d \\ \dfrac{P_{oc}(t)}{P_b(t)} = 1 + \dfrac{R_b P_{oc}(t)}{V_{oc}^2 - R_b P_{oc}(t)}, & \text{otherwise} \end{cases} \quad (17)$$

The following assumptions are also made to address the fundamental analysis.

Assumption 1: The ICE is large enough, such that $P_{PS_{\max}} \ge \sup\{P_{PL}(t)\}$ holds for a given driving cycle.

Assumption 2: Given a driving cycle, the charge sustaining condition (15) is reachable, such that the total regenerated battery charge during the time interval Ψ (obtained by following (16) and the second equation in (3))

$$\Delta_\Psi \mathrm{SOC} = \int_\Psi \frac{P_{PL}(t)\eta_{dc}\eta_b(t)}{V_{oc}Q_{\max}} dt, \quad (18)$$

satisfies the condition

$$-\Delta_\Psi \mathrm{SOC} \le \int_\Phi \frac{\min(P_{PL}(t), P_{SS_{\max}})}{\eta_{dc}\eta_b(t)V_{oc}Q_{\max}}\, dt\,, \quad (19)$$

where the right hand side of (19) represents the maximum possible battery discharge throughout the mission (during the time interval Φ).

Assumption 3: The battery is properly sized and SOC

operational limits $\mathrm{SOC}_{\min}$ and $\mathrm{SOC}_{\max}$ are selected, such that SOC constraints (11) are not violated throughout the mission when the forthcoming analytic solution is employed.

Assumption 1 is naturally fulfilled for a non-plug-in HEV, which is expected to have a sufficiently large engine, allowing the vehicle to be continuously driven under ICE-only mode. The inequality condition (19) assumed in Assumption 2 is expected to be true as: 1) in a normal driving cycle on a level road the positive (driving) wheel energy is larger than the negative (braking) wheel energy due to the various energy losses throughout the mission, and 2) the HEV battery allows much larger discharging power than charging power, such that $|P_{SS_{\max}}|>|P_{SS_{\min}}|$ (e.g., A123 AHR32113 cell allows 30C for discharging while only 4C for charging). Assumption 3 may be strong, but HEVs are expected to be designed for the intended missions with large enough batteries to avoid deep charges/discharges that rapidly wear the battery out. Hence, it is reasonable to assume that the SOC is always operated within the selected range.

A. Analytic Solution

By integrating both sides of the FCM (shown in (10)) over $[0,\, T]$ and applying (8), we obtain:

$$m_f(t) = m_{f0}(t) - \alpha_f \int_{\Phi} \eta_{dc}^{\mathrm{sign}(P_b)(t)} P_b(t)\, dt, \tag{20}$$

where $m_{f0}(t) = q_{f0}T + \alpha_f \int_{\Phi} P_{PL}(t)dt$ is a fixed term, independent of the EM control. By using the definitions of Φ_d and Φ_c, (20) can be expanded as follows:

$$m_f(t)=m_{f0}(t) - \alpha_f \left(\eta_{dc} \int_{\Phi_d} P_b(t)dt + \frac{1}{\eta_{dc}} \int_{\Phi_c} P_b(t)dt\right) \tag{21}$$

Due to the fact that

$$\int_{\Phi_c} P_b dt \leq 0, \quad \int_{\Phi_d} P_b dt \geq 0, \quad \eta_{dc} < 1,$$

$m_f(t)$ is minimized when $\int_{\Phi_c} P_b dt = 0$ and $\int_{\Phi_d} P_b(t)dt$ is maximized. The former condition further implies that $P_b(t)=0,\ \forall t \in \Phi_c$. As such, $\Phi_c = \emptyset$ and $\Phi_d = \Phi$ indicating that for an optimal EM the SS is never charged directly by the PS throughout the whole mission. This solution also implies that the battery is only charged by regenerative braking, which produces a fixed amount Q_+ of battery charge for a given driving cycle:

$$Q_+ = -Q_{\max} \Delta_\Psi \mathrm{SOC} \tag{22}$$

where $\Delta_\Psi \mathrm{SOC}$ is defined in (18). On the other hand, the term $\int_{\Phi_d} P_b(t)dt$ can be rewritten by using (17), as follows:

$$\int_{\Phi_d} \eta_b(t) P_{oc}(t)dt = \int_{\Phi} \left(1 - \frac{R_b}{V_{oc}^2} P_{oc}(t)\right) P_{oc}(t)dt\,. \tag{23}$$

By considering the charge sustaining condition $\Delta\mathrm{SOC} = 0$ in (15), which implies:

$$\int_{\Phi} P_{oc}(t)dt - V_{oc}Q_+ = 0, \tag{24}$$

the right hand side of (23) can be further simplified to:

$$V_{oc}Q_+ - \frac{R_b}{V_{oc}^2} \int_{\Phi} P_{oc}(t)^2 dt\,.$$

Therefore, it is immediate to construct the following optimization problem by which m_f is minimized:

$$\min_{P_{oc}} \int_{\Phi} P_{oc}(t)^2 dt, \tag{25}$$

subject to constraints (24) and (14). The latter constraint can be simplified to $P_{oc}(t) \leq P_{oc_{\max}}(t)$, where $P_{oc_{\max}}(t)$ is the power limit of $P_{oc}(t)$. The justification for this simplification (for the Φ time interval) is as follows. Since $\Phi_c = \emptyset$, then $P_{SS}(t) \geq 0$ is always true. Also, on the basis of Assumption 1, $\max(P_{PL}(t) - P_{PS_{\max}},\, P_{SS_{\min}}) \leq 0$. Hence, the first part of (14) is guaranteed. Regarding the second part of (14), by resorting to the relationship between P_{SS} and P_{oc} during the time interval Φ_d (see (8) and (17)),

$$P_{SS}(t) = \eta_{dc}\eta_b(t) P_{oc}(t), \tag{26}$$

and therefore, $P_{oc}(t) \leq \frac{\min(P_{SS_{\max}}, P_{PL}(t))}{\eta_{dc}\eta_b(t)}$, in which,

$$\frac{\min(P_{SS_{\max}}, P_{PL}(t))}{\eta_{dc}\eta_b(t)} = P_{oc_{\max}}(t). \tag{27}$$

By discretizing $P_{oc}(t)$ over the time interval Φ at N time instants $t_1, t_2, \cdots, t_N$ with a fixed sampling time T_s, and denoting $P_{oc}(k)$ the sample at t_k, the problem (25) can be converted into a constrained optimization problem:

$$\min_{P_{oc}} \sum_{k=1}^{N} P_{oc}(k)^2$$

subject to

$$\sum_{k=1}^{N} P_{oc}(k)T_s - V_{oc}Q_+ = 0 \quad \text{and} \quad P_{oc}(k) \leq P_{oc_{\max}}(k). \tag{28}$$

Such an optimization problem can be easily solved by using the Karush-Kuhn-Tucker (KKT) optimality condition, ending up with a solution:

$$P_{oc}(k) = P_{th}, \qquad \text{if } P_{oc_{\max}}(k) \geq P_{th} \tag{29a}$$
$$P_{oc}(k) = P_{oc_{\max}}(k), \quad \text{if } P_{oc_{\max}}(k) < P_{th} \tag{29b}$$

where P_{th} is a constant power threshold depending on $V_{oc}Q_+$, and consequently on Δ_ΨSOC. By considering Assumption 2, it can be inferred that $\frac{P_{SS_{\max}}}{\eta_{dc}\eta_b(t)} \geq P_{th}$, and therefore $P_{SS_{\max}}$ can be dropped from the expression of $P_{oc_{\max}}(t)$ in (27), since $P_{oc}(t) \leq \frac{P_{SS_{\max}}}{\eta_{dc}\eta_b(t)}$ is guaranteed. Consequently,

$$P_{oc_{\max}}(t) = \frac{P_{PL}(t)}{\eta_{dc}\eta_b(t)}, \tag{30}$$

and the solution (29) can be rewritten as follows:

$$P_{oc}(k) = P_{th}, \qquad \text{if } P_{PL}(k) \geq P_{th}\eta_b(k)\eta_{dc} \tag{31a}$$
$$P_{oc}(k) = \frac{P_{PL}(k)}{\eta_{dc}\eta_b(k)}, \quad \text{if } P_{PL}(k) < P_{th}\eta_b(k)\eta_{dc} \tag{31b}$$

By applying (26), the condition (31) can be rewritten in terms of P_{SS}:

$$P_{SS}(k) = P_{SS,th}, \quad \text{if } P_{PL}(k) \geq P_{SS,th} \tag{32a}$$
$$P_{SS}(k) = P_{PL}(k), \quad \text{if } P_{PL}(k) < P_{SS,th} \tag{32b}$$

where $P_{SS,th}=\eta_{dc}\left(1-\frac{R_b}{V_{oc}^2}P_{th}\right)P_{th}$. Note that the case when $P_{PL}(t)<0$ (see (16)) is naturally incorporated by (32b).

This solution is remarkable since it simply suggests that an EM strategy is optimal in terms of fuel consumption if the following conditions are met: 1) the SS is never charged directly by the PS throughout the whole mission, and 2) the SS is operated at a load following fashion when P_{PL} is smaller than the power threshold, otherwise P_{SS} follows a fixed threshold that depends on Δ_ΨSOC (see (18)).

B. Truncated Battery Power Following Strategy (TBFS)

Inspired by the preceding solutions, the TBFS is developed and graphically shown in Fig. 4. As it can be noticed, the

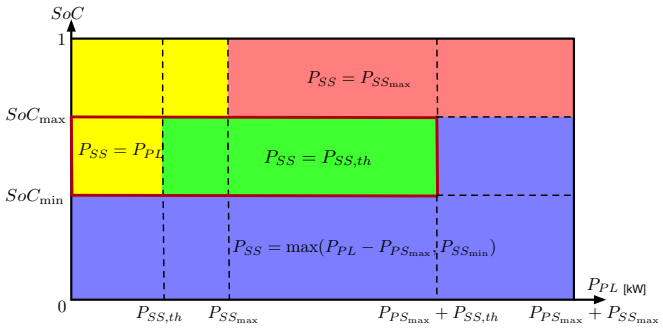

Fig. 4. The operation scheme of the TBFS with different operating stages classified based on the given SOC and P_{PL}.

principles of TBFS are defined based on a 2-dimensional map of the SOC and P_{PL}, which is partitioned into several zones by the SOC limits and power load thresholds. The primary operation mode is activated in the zones where the coordinates (on the P_{PL}-SOC map) satisfy $\text{SOC}_{\min} \leq \text{SOC} \leq \text{SOC}_{\max}$ and $0 \leq P_{PL} \leq P_{PS_{\max}} + P_{SS,th}$, which give rise to a rectangular box on the plane (see the box with solid and red frame). The optimality condition (32) is rigorously followed within this mode. Any coordinate outside the primary region triggers the emergency rules, which essentially enforce the SOC to be sustained and define the power split for extremely large power demand. It is worth pointing out that the emergency handling rules provide no fuel efficiency guarantee, and they are requested to deal with exceptional driving circumstances only.

Compared to the XOS [14], the TBFS also operates in the SS-only mode at lower power demands ($P_{PL} \leq P_{SS,th}$). However, the TBFS switches to a hybrid model when P_{PL} further increases rather than the PS-only mode adopted by the XOS. The power threshold $P_{SS,th} > 0$ that determines when to switch from SS-only mode to hybrid mode represents the only design parameter of the TBFS. For a given driving cycle, the tuning process of $P_{SS,th}$ is based on a simple parameter searching approach, which ends when the charge sustaining condition (15) is reached. In this context, if none of the emergency rules is triggered during the driving mission, the analytic solution (32) is realized without solving any optimization.

IV. Numerical Results

A. Driving Cycles

The driving cycle defines the speed profile that needs to be followed by the vehicle, it thus heavily influences the operation of the EM strategy and the overall fuel economy. In this work, the proposed TBFS will be globally tuned for the WLTP speed profile that corresponds to the latest test procedure adopted by industry. As shown in Fig. 5, the WLTP profile is a single driving cycle with four stages, defined by their speed: low (WL-L), medium (WL-M), high (WL-H) and extra high (WL-E). Each of the stages can be considered on their own as independent driving cycles. Some particular features of the selected speed profiles are specified in Table II.

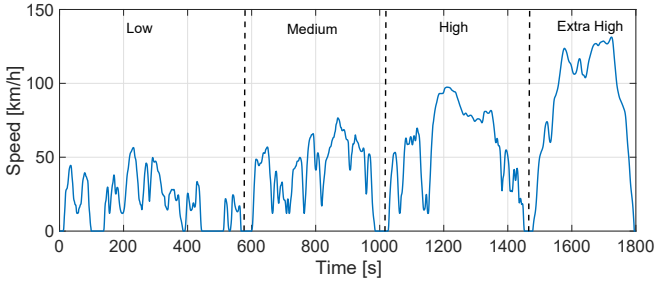

Fig. 5. Speed profile of the WLTP with four different stages according to the average speed.

TABLE II
Characteristics of WLTP speed profiles

	WL-L	WL-M	WL-H	WL-E
Duration [s]	589	433	455	323
Distance [km]	3.1	4.8	7.2	8.3
Average Speed [km/h]	18.9	39.5	56.6	92
Max speed [km/h]	56.5	76.6	97.4	131.3
Max accel. [m/s^2]	1.47	1.57	1.58	1.03
Max decel. [m/s^2]	-1.47	-1.49	-1.49	-1.21

B. Simulation Examples

The behavior of the proposed TBFS is investigated in this Section. The control policies of the TBFS are obtained by tuning the parameter $P_{SS,th}$ for each of the four driving cycles of the WLTP profile. The tuning process ends up with: $P_{SS,th} = 3.17\,\text{kW}$ for the WL-L, $P_{SS,th} = 3.27\,\text{kW}$ for the WL-M, $P_{SS,th} = 2.11\,\text{kW}$ for the WL-H and $P_{SS,th} = 1.72\,\text{kW}$ for the WL-E, by which the charge sustaining condition (15) is guaranteed in all scenarios. For benchmarking purposes, the DP algorithm developed in [18] is implemented. To ensure a high level of accuracy, the state variable SOC and the control input P_{SS} are finely gridded with 400×2000 points over the admissible ranges $[\text{SOC}_{\min}, \text{SOC}_{\max}] \times [P_{SS_{\min}}, P_{SS_{\max}}]$. The sampling times used in both methods are identical, $T_s = 0.5$s.

It has been found that in all driving cycle cases Assumptions 1-3 are satisfied. As such, the emergency handing rules are not triggered and the TBFS strictly obeys the optimality condition (32). Consequently, the TBFS highly resembles the global optimal solutions found by DP for all tested cycles. In Figs. 6-7, two examples of the resulting power profiles of DP and the TBFS when driving the WL-M and WL-E are illustrated. As it can be seen, the battery is never charged by the engine, and the charge sustaining condition is reached by depleting all the regenerated charge for propulsion by the end of the missions, as described by the analytic results. The SOC profiles for both cases are shown in Fig. 8, which further confirm the effectiveness of the TBFS in emulating the global optimal solutions. Finally, the simulation shows that the tuning of TBFS on average saves about 80% of computation time as compared to the DP optimization.

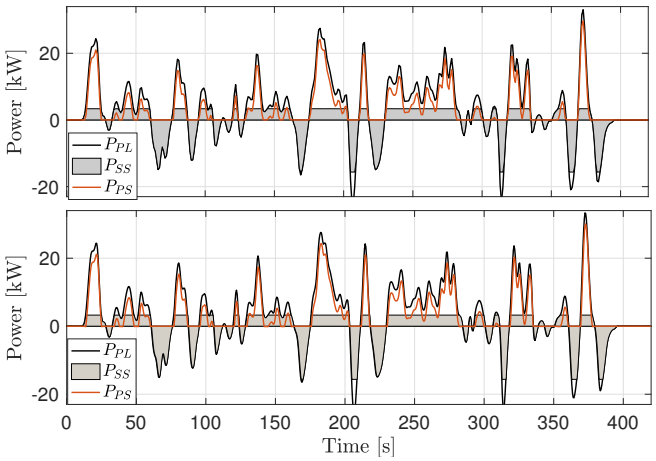

Fig. 6. Power profiles solved by DP (top) and TBFS (bottom) when driving the WL-M driving cycle.

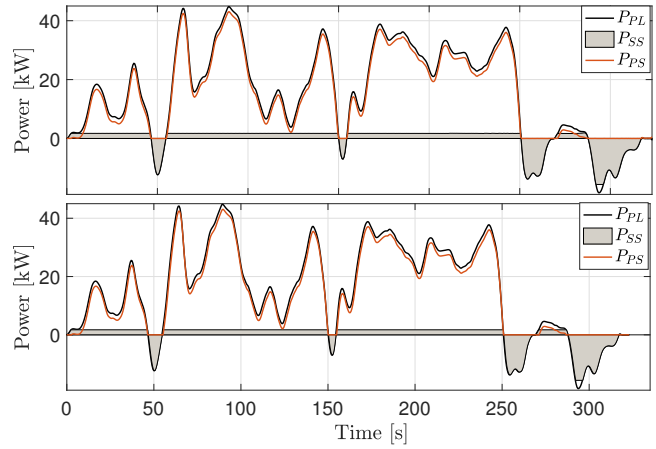

Fig. 7. Power profiles solved by DP (top) and TBFS (bottom) when driving the WL-E driving cycle.

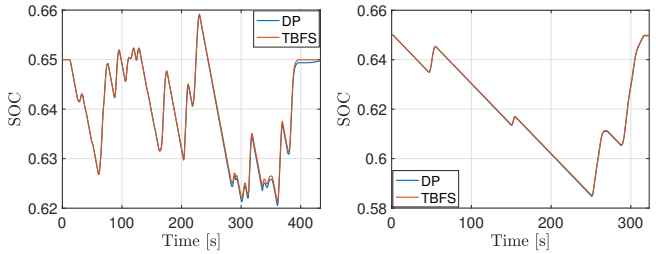

Fig. 8. Battery SOC profiles solved by DP and TBFS when driving the WL-M (left) and WL-E (right) driving cycles.

V. Conclusions

This paper proposes a novel rule-based energy management (EM) control strategy for series hybrid electric vehicles (HEVs), the truncated battery power following strategy (TBFS). The fundamental control rules are extracted from the mathematical analysis of a simple but representative vehicle model, in which the engine fuel mass rate is linearly related to the primary source power. Thus, it is possible to arrive at feasible fundamental optimization solutions that take into account the main physics of the energy management problem for series HEVs. The TBFS essentially combines two operational modes: battery-only mode and hybrid mode, which are separated by the designed power threshold. This parameter is regulated based on the information of the driving cycle, targeting charge sustaining operation. As such, the globally optimal solutions for the presented vehicle model can be simply produced by the TBFS without referring to dynamic programming (DP), which usually involves heavy computation effort. The simple nature of the TBFS also makes it a potential benchmark strategy for high-fidelity vehicle models, where DP is not applicable any more. Future work involves extending TBFS to incorporate driving speed prediction, which may allow the TBFS to be implemented in real-time.

References

[1] A. A. Malikopoulos, "Supervisory power management control algorithms for hybrid electric vehicles: A survey," *IEEE Transactions on Intelligent Transportation Systems*, vol. 15, no. 5, pp. 1869–1885, 2014.

[2] C. M. Martinez, X. Hu, D. Cao, E. Velenis, B. Gao, and M. Wellers, "Energy management in plug-in hybrid electric vehicles: Recent progress and a connected vehicles perspective," *IEEE Transactions On Vehicular Technology*, vol. 66, no. 6, pp. 4534–4549, 2017.

[3] L. V. Pérez and E. A. Pilotta, "Optimal power split in a hybrid electric vehicle using direct transcription of an optimal control problem," *Math. and Comput. in Simulation*, vol. 79, no. 6, pp. 1959–1970, February 2009.

[4] Y. L. Murphey, J. Park, Z. Chen, M. L. Kuang, M. A. Masrur, and A. M. Phillips, "Intelligent hybrid vehicle power control — part i: Machine learning of optimal vehicle power," *IEEE Transactions On Vehicular Technology*, vol. 61, no. 8, pp. 3519–3530, 2012.

[5] Y. L. Murphey, J. Park, L. Kiliaris, M. L. Kuang, M. A. Masrur, A. M. Phillips, and Q. Wang, "Intelligent hybrid vehicle power control — part ii: Online intelligent energy management," *IEEE Transactions On Vehicular Technology*, vol. 62, no. 1, pp. 69–79, 2013.

[6] A. Sciarretta and L. Guzzella, "Control of hybrid electric vehicles," *IEEE Transactions on Control Systems Technology*, vol. 27, no. 2, pp. 60–70, 2007.

[7] J. Zhang and T. Shen, "Real-time fuel economy optimization with nonlinear MPC for PHEVs," *IEEE Transactions On Control Systems Technology*, vol. 24, no. 6, pp. 2167–2175, 2016.

[8] B. Chen, S. Evangelou, and R. Lot, "Fuel efficiency optimization methodologies for series hybrid electric vehicles," in *IEEE Vehicle Power and Propulsion Conference (VPPC)*, 2018.

[9] Y. Zhang, H. Liu, and Q. Guo, "Varying-domain optimal management strategy for parallel hybrid electric vehicles," *IEEE Transactions On Vehicular Technology*, vol. 63, no. 2, pp. 603–616, 2014.

[10] B. Chen, S. Evangelou, and R. Lot, "Impact of optimally controlled continuously variable transmission on fuel economy of a series hybrid electric vehicle," in *IEEE Proceedings of the European Control Conference*, Limassol, Cyprus, 2018.

[11] W. Zhou, C. Zhang, J. Li, and H. K. Fathy, "A pseudospectral strategy for optimal power management in series hybrid electric powertrains," *IEEE Transactions On Vehicular Technology*, vol. 65, no. 6, pp. 4813–4825, 2016.

[12] S. Uebel, N. Murgovski, C. Tempelhahn, and B. Baker, "Optimal energy management and velocity control of hybrid electric vehicles," *IEEE Transactions On Vehicular Technology*, vol. 67, no. 1, pp. 327–337, 2018.

[13] L. Serrao, S. Onori, and G. Rizzoni, "A comparative analysis of energy management strategies for hybrid electric vehicles," *Journal of Dynamic Systems, Measurement, and Control*, vol. 133, 2011.

[14] W. Shabbir and S. A. Evangelou, "Exclusive operation strategy for the supervisory control of series hybrid electric vehicles," *IEEE Transactions On Control Systems Technology*, vol. 24, no. 6, pp. 2190–2198, 2016.

[15] R. Lot and S. A. Evangelou, "Green driving optimization of a series hybrid electric vehicle," in *IEEE Conference on Decision and Control*, 2013, pp. 2200–2207.

[16] L. Serrao and G. Rizzoni, "Optimal control of power split for a hybrid electric refuse vehicle," in *IEEE Proceedings of the American Control Conference*, 2008, pp. 4498–4503.

[17] T. Markel, A. Brooker, T. Hendricks, V. Johnson, K. Kelly, B. Kramer, M. O'Keefe, S. Sprik, and K. Wipke, "Advisor: a systems analysis tool for advanced vehicle modeling," *Journal of Power Sources*, vol. 110, no. 2, pp. 255–266, 2002.

[18] P. Elbert, S. Ebbesen, and L. Guzzella, "Implementation of dynamic programming for n-dimensional optimal control problems with final state constraints," *IEEE Transactions on Control Systems Technology*, vol. 21, no. 3, pp. 924–931, 2013.